

# Nano-scale morphology dependent performance of thin film organic solar cells

Mireille M. Tchoukouegno<sup>1</sup> · Giuseppe Pellicane<sup>1</sup> ·  
Mesfin Tsige<sup>2</sup> · Genene Tessema Mola<sup>1</sup>

Received: 8 July 2016 / Accepted: 8 August 2016 / Published online: 16 August 2016  
© Springer Science+Business Media New York 2016

**Abstract** Polymer-fullerene based thin film organic solar cells (TFOSC) composed of poly(3-hexylthiophene) donor and [6,6]-phenyl-C<sub>61</sub>-butyric acid methyl ester electron acceptor are investigated with and without different processing additives such as: 1,8-diiodooctane (DIO), 1-chloronaphthalene and dimethyl sulfoxide (DMSO). The effect of these solvents on device performance has been investigated and discussed in terms of changes in optical, electrical and microstructural properties of the photoactive films. Among the additives used in this study DIO has shown remarkable effect on preventing the formation of defect related clusters in the medium and assists the crystallization of the polymer chain leading to the best device performance in the investigation. The nanoscale structures of the films produced with DMSO showed the presence of large concentration of defect clusters resulting in poor performance. Various results of TFOSC devices with and without solvent additives are compared and thoroughly discussed.

## 1 Introduction

One of the main challenges in rapidly growing population of the world today is to satisfy the increasing demand for energy. Fossil fuels have been the main source of energy at

present which is causing grave consequences to the very existence of life in our planet. In fact, environmental pollution is the main factor that calls for a decreasing dependency on fossil fuels. The imperative of looking for alternative energy sources, as dictated by the rapidly approaching energy shortfall, has boosted research in solar energy conversion. Solar power based on crystalline silicon technology is not economically competitive with fossil fuels. Therefore, the search for cheaper renewable sources of energy has motivated organic electronics research based on conducting polymers. Especially, organic solar cells have been given immense attention due to their potential for low cost device production, flexibility, integrability and ease of processability [1–9]. However, the fast degradation of the organic molecules under ambient environmental conditions has been the major challenges that is slowing the realization of organic photovoltaic in the energy market [6–13]. Moreover, a power conversion efficiency (PCE) of 10% or more is regarded as an important threshold for large-scale production of polymer solar cells.

A number of investigations employing suitable buffer layers, mixed solvents and thermal annealing have been performed to optimize the phase separation between donor and acceptor molecules in the photoactive medium with the view to improve device performance by inducing crystallization in the donor molecules domain. Numerical studies using computer simulations were able to provide important information on phase separation and crystallization process for a number of soft-matter systems [14, 15]. In addition, it has been reported that morphology of the BHJ active layer in polymer solar cells (PSCs) can be modified using mixed solvents and processing solvent additives which have different boiling points to reduce preferential phase segregation in the blend [2, 16, 17]. An investigation by Zhang et al. [16], recorded significant

✉ Genene Tessema Mola  
mola@ukzn.ac.za

<sup>1</sup> School of Chemistry and Physics, University of KwaZulu-Natal, Pietermaritzburg Campus, Private Bag X01, Scottsville 3209, South Africa

<sup>2</sup> Department of Polymer Science, University of Akron, Akron, OH 44325, USA

improvement in  $J_{sc}$  from 3.2 to 5.2 mA/cm<sup>2</sup> using APFO-3:PC<sub>61</sub>BM blend solar cell by adding a small amount of chlorobenzene into a chloroform solution due to the formation of a more homogeneous nanomorphology [16]. On the other hand, Peet et al. [18] reported that the efficiency of the PCPDTBT:PC<sub>71</sub>BM solar cell improved from 2.8 to 5.5 % by using alkane dithiols as processing solvents additive [18]. Both reports indicated that solvent additives are beneficial for active layer morphology, and since then, processing solvent additives have been widely used in the nanoscale morphological modification [1, 2, 16]. Lee et al. [19–21] proposed two criteria for choosing the processing solvent additive in optimizing the nano-morphology of the BHJ active layer: (1) the polymer and the fullerene derivative should show selective solubility in the solvent additive; (2) the boiling point of the solvent additive needs to be higher than that of the host solvent. For instance, in P3HT:PCBM blend active layer the crystallization of the P3HT phase can be inhibited by the clustering of fullerene during annealing of the film. This effect could be avoided by using a high boiling point solvent additive with selective solubility for fullerene thereby allowing increased crystallinity of the P3HT without disruption by fullerene during thermal treatment [22, 23]. The SEM images taken from P3HT:PC<sub>61</sub>BM active layer showed that indeed the processing solvent additive 1, 8-diiodooctane, delayed the process of drying the film, which gave more time for P3HT to crystallize. Likewise, the processing solvent additive was found to improve the morphology of the active layer based on PCPDTBT:PC<sub>71</sub>BM via improving the aggregation of the polymer [24].

In this paper, we focus on polymer-fullerene BHJ organic solar cells composed of P3HT and PCBM blend. Since the device performance is critically dependent on the nano-scale morphology of the photoactive medium, this investigation is aimed at improving the film morphology by employing solvent additives which selectively dissolve the fullerene in the blend solution. We used DIO, CN, and DMSO, whose boiling points are 168, 259 and 189 °C, respectively. The device performances of the the films with additives are compared with the reference cell (without additives) produced under the same environment. The host solvent in the preparation of TFOSC devices was chloroform which has a boiling point of 61.2 °C lower than all processing solvent additives used in this study. The effectiveness of the additives will be examined in terms of measurable changes in optical, electrical and structural properties of the P3HT:PCBM films prepared with and without solvent additives. Each of these properties will be discussed in details in the Sect. 3 including the charge transport properties of the device.

## 2 Materials and methods

The materials used in the preparation of bulk heterojunction organic solar cell devices were obtained from various chemical suppliers. Poly(3,4-ethylenedioxythiophene):poly(styrenesulfonate) (PEDOT:PSS), poly(3-hexylthiophene-2,5-diyl) (P3HT), [6,6]-phenyl C61-butyric acid methyl ester (PCBM) and indium thin oxide (ITO) coated glass substrate were purchased from Oscilla Ltd and used as received. 1,8-diiodooctane (DIO), 1-chloronaphthalene (CN) and dimethyl sulfoxide (DMSO) were purchased from Sigma Aldrich and used as received. The solution of the photoactive layer composed of P3HT and PCBM blend at 1:1 ratio by weight was prepared in chloroform solvent at concentration of 20 mg/ml. Four types of solutions were prepared; one without additive and three others with additives such as DIO, CN and DMSO, respectively. The DIO and CN were used 3 % by volume with chloroform (CF) host solvent, however, we used 1, 3 and 10 % DMSO by volume with respect to CF. The organic solar cells were fabricated on ITO coated glass substrates (30 cm × 30 cm) which were partially etched using acid solution containing 48 %HCl:48H<sub>2</sub>O:4 %NHO<sub>3</sub> by volume. The substrates were then cleaned by ultrasonic bath using deionized water, acetone and isopropanol for 10 min each, respectively. The substrates were then dried in an oven at 120 °C for 10 min holding time. The hole transport layer (PEDOT:PSS) were spin coated on each substrate at 3500 rpm and followed by annealing in nitrogen (N<sub>2</sub>) filled atmosphere at 120 °C for 10 min. This buffer layer assures better hole mobility from the polymer to the ITO electrode. PEDOT:PSS also prevents any possible short circuiting due to the ITO spikes and pin holes. The photoactive layers were spin coated from the solution at 1200 rpm on top of the PEDOT:PSS layer. After holding the samples for nearly 5 min at 70 °C in nitrogen filled furnace, they were then immediately transferred into a vacuum deposition chamber for the counter electrode deposition. The lithium fluoride (LiF) buffer layer and aluminium (Al) electrodes were deposited sequentially at 0.4 and 50 nm, respectively, in vacuum ( $\approx 2 \times 10^{-6}$  mbar). The active region of the diodes formed by the deposition mask ranges between 0.03 and 0.05 cm<sup>2</sup>. Optical absorption of the films were measured using double beam UV/VIS spectrophotometer (Model: UV-1601). The electrical properties of the devices were taken using computer interfaced Keithley HP2400 source-meter both under illumination and dark condition. The solar simulator (model SS50AAA) and AM1.5 used was operating at an integrated power intensity of 100 mW/cm<sup>2</sup>. To investigate the variation of in-plane morphology induced by solvent mixing, the scanning electron microscope (SEM) (Zeiss crossbeam series with Gemini FESEM) was used.

### 3 Results and discussion

Bulkheterojunction thin film organic solar cells based on P3HT:PCBM were fabricated with and without solvent additives. We employed chloroform as host solvent and a small quantity of additives DIO, CN and DMSO were used in the solution of the photoactive medium. We employed sandwich type structure consisting of a sequence of layers such as ITO/PEDOT:PSS/P3HT:PCBM/LiF/Al in the device preparation. Results found from optical and electrical measurements of TFOSC as well as the morphology of the photoactive films of the devices are presented and discussed below.

#### 3.1 Optical absorption

The optical absorption spectra of P3HT:PCBM blend films coated on glass substrates were taken with and without additives. Fig. 1 shows the optical properties of the absorption spectra for, four different P3HT:PCBM blend preparation conditions one without additive and three of which were either with DIO, CN or DMSO processing solvent additives. According to the measured spectra, all the thin films had the absorption bands extending over the range of 420–650 nm. However, the devices containing DIO exhibited the highest absorption coefficient whose peak absorbance is concentrated within 450–620 nm, while the other two thin films (with CN and without additive) have apparently lower peak but similar characteristics over the same range of wavelengths. The spectrum taken from the film with DMSO shows a flat band with no sign of any absorbance. The stronger absorption observed in the device containing DIO solvent additive could be attributed to the more ordered structure of P3HT, which is the reason for enhanced photocurrent in the devices.

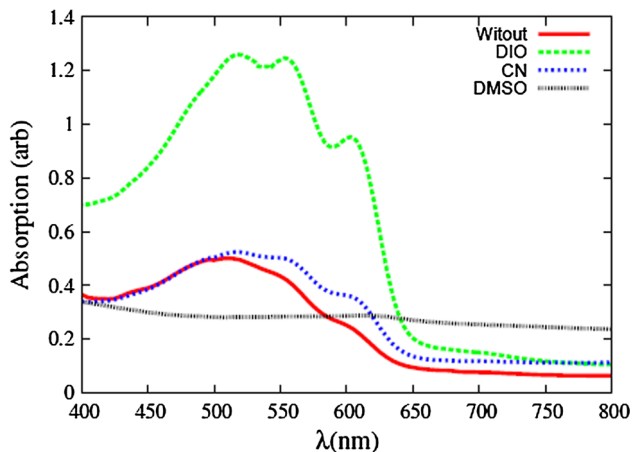


**Fig. 1** Optical absorption spectra of three different organic active layers of P3HT:PCBM blend fabricated with and without different solvent additives

#### 3.2 Electrical properties of the devices

##### 3.2.1 P3HT:PCBM without solvent additive

The reference sample in this study was prepared from the solution containing P3HT:PCBM blend in chloroform host solvent without any processing additives. The photoactive layer was spin coated on top of PEDOT:PSS coated substrate at 1200 rpm. The current–voltage characteristics given in Fig. 2 clearly shows the nonlinear nature of the current output. The J–V curve taken under illumination shows a very good device rectification property as it can be seen from the uniformity of the result and large fill factors (see Table 1). The measured fill factors are reasonably good under ambient laboratory preparation condition, however, the observed high series resistance of the devices seriously affect the shape of the J–V curves under illumination as reported in Fig. 2. The open circuit voltage ( $V_{oc}$ ) and short circuit current ( $J_{sc}$ ) measured are comparable with the data reported in literatures [12]. The mean values of the device parameters measured from this experiment are PCE = 1.88, FF = 43 and  $V_{oc}$  = 570 mV. The space

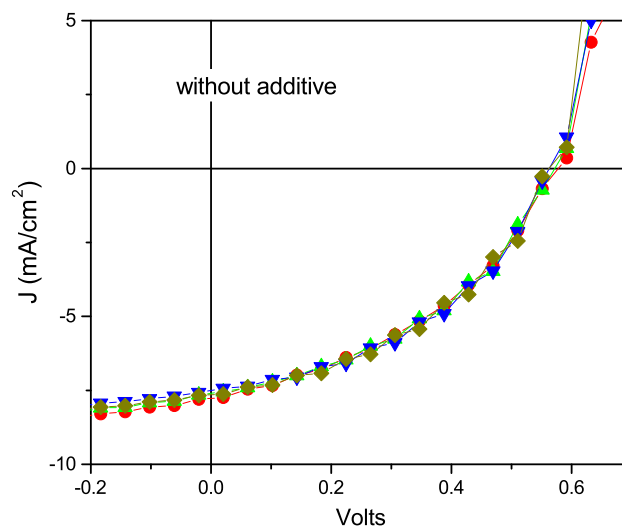


**Fig. 2** J–V characteristics of organic thin film solar cell devices based on the blend of P3HT:PCBM active layer prepared without additive under illumination

**Table 1** Photovoltaic parameters of best performed diodes of organic thin film solar cell devices based on the blend of P3HT:PCBM active layer prepared without additive

Diodes	$V_{oc}$ (V)	$J_{sc}$ (mA/cm <sup>2</sup> )	FF (%)	PCE (%)	$R_s$ (ohms)
d1	0.58	7.8	40	1.81	601
d2	0.57	7.6	43	1.88	442
d3	0.56	7.5	45	1.93	418
d4	0.56	7.7	44	1.89	630

charge limiting current were found to be similar for all the diodes as reported in the bottom right hand panel of Fig. 2.

### 3.2.2 P3HT:PCBM with 3% DIO

Devices were also fabricated using the same P3HT:PCBM blend in chloroform solvent with 3 % by volume of a 1, 8-diiodooctane (DIO) processing solvent additive in the solution. The solution was then sonicated for 3 h to allow homogeneity and inter-dispersion of the molecules. The photoactive layer was spin coated on PEDOT:PSS coated substrate at 1200 rpm in the standard device preparation. The current–voltage characteristics measured from the devices were indicating a good photovoltaic performance with large photocurrent and fill factors (see Fig. 3). The shape of the J–V curve shows good rectification of the diodes leading to the large fill factor compared to the reference solar cell. The maximum short circuit current and fill factor measured from this TFOSC were  $J_{sc} = 11.4 \text{ mA/cm}^2$  and 60 %, respectively (see Table 2). Generally, the device performances for the active layers with DIO additive found to be much better than those prepared without an additive. The mean value of power conversion efficiency (PCE),  $J_{sc}$  and fill factor are 2.73 %,  $10.7 \text{ mA/cm}^2$  and 55 %, respectively. These are reasonable values of device parameters found from device preparation

in an open laboratory environment without glove box or clean room. However, the measured open circuit voltages here are relatively low compared with the reference solar cell which could be attributed to the modification of the work function of ITO electrode due to its interaction with DIO solvent [18, 21].

### 3.2.3 P3HT:PCBM with 3% CN

The effect of 1-chloronaphthalene (CN) in thin film organic solar cell is investigated by adding 3 % processing solvent additive CN in chloroform based solution of P3HT:PCBM. The J–V characteristics as depicted in the bottom panel of Fig. 3 clearly show a typical device properties of thin film organic solar cell. Unlike the previous two types of devices discussed above, the performance of CN doped films was not uniform which can be seen from the shape of the the J–V curves as well as the values of  $J_{sc}$  and fill factor (reported in Table 2). The dissimilarity of these values suggest that the active layer medium might have not been homogenous through out the film. This could be attributed to the higher boiling point of CN ( $250^\circ\text{C}$ ) which results in moderate morphology formation of the polymers molecules. The overall performance of the devices lay between those devices without additive and with DIO. The average value of the device parameters were 0.55 V,  $8.63 \text{ mA/cm}^2$ , 50 and 2.34 % for  $V_{OC}$ ,  $J_{sc}$ , FF and PCE, respectively. However, the maximum power conversion efficiency recorded was 2.86 % higher than any of the devices produced so far. Generally, the device with CN additive exhibited higher

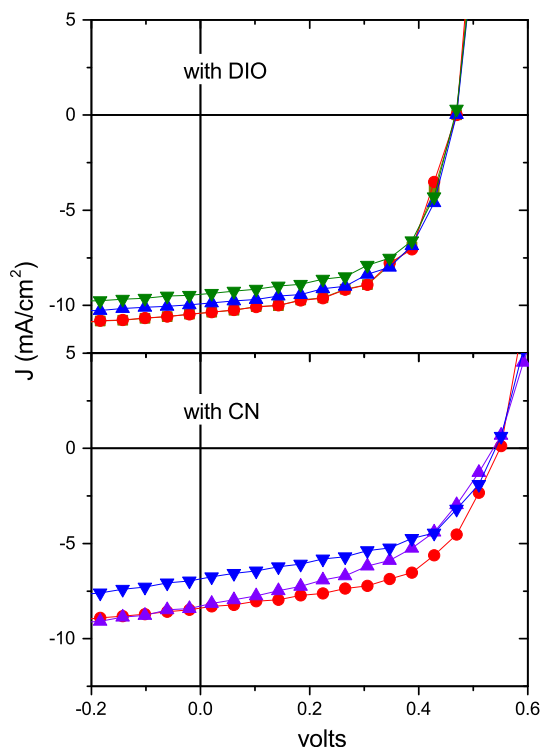


**Fig. 3** J–V characteristics of thin film organic solar cell devices based on P3HT:PCBM active layer prepared with DIO (*top panel*), CN (*middle panel*) and DMSO (*bottom panel*) solvent additives

**Table 2** Best photovoltaic device parameters of thin film organic solar cells based on P3HT:PCBM active layer with DIO, CN and DMSO processing solvent additive

	$V_{oc}$ (V)	$J_{sc}$ ( $\text{mA/cm}^2$ )	FF (%)	PCE (%)	$R_s$ (ohms)
<i>Diodes with DIO</i>					
d1	0.47	11.4	51	2.70	105
d2	0.47	11.2	51	2.74	95
d3	0.47	10.4	56	2.75	59
d4	0.47	9.91	60	2.77	176
<i>Diodes with CN</i>					
d1	0.54	6.9	51	1.91	536
d2	0.55	10.7	49	2.86	671
d3	0.55	8.4	55	2.54	877
d4	0.54	8.5	45	2.05	699
<i>Diodes with DMSO</i>					
d1	0.662	0.0350	13.752	0.0032	68,981
d2	0.612	0.0356	15.019	0.0033	213,740
d3	0.582	0.0345	15.282	0.0031	123,135
d4	0.663	0.0388	14.244	0.0037	89,168

series resistance compared to DIO based devices which results in reduction of short circuit current and PCE.

### 3.2.4 P3HT:PCBM with DMSO

Thin film organic solar cells were fabricated using DMSO as solvent additive in chloroform based P3HT:PCBM solution. We have tested various quantity of DMSO by volume in host solvent such as 1, 3 and 10 % but in all cases the results turned into unexpected direction for reasons which are not clear at the moment. The current–voltage characteristics of the TFOSC show poor device rectification as well as high series resistances in all devices fabricated with DMSO. DMSO has been reported to be a good solvent additive in the preparation of TFOSC, however, inspite of applying the recommendations and procedures provided in literatures, the effect of DMSO in our samples found to be negative. The measured average device parameters are  $J_{sc} = 0.035 \text{ mA/cm}^2$ ,  $\text{FF} = 15 \%$ ,  $\text{PCE} = 0.003 \%$  which are very low compared to the other processing additives discussed in the last sections. On the other hand, the  $V_{oc}$  is 0.6 V which is higher than the one obtained from DIO and CN additives. DMSO has unique properties that are suitable to be used as processing solvent additive; this includes, nonreacting materials with either the polymer or fullerene; selective solubility of one of the molecule from the polymer blend and, higher boiling point than the host solvent. The observed appalling results could be attributed to the fact that DMSO is the “secondary dopant” which is usually used as anodic buffer layers mainly used to improve the morphology and conductivity of the PEDOT:PSS buffer layer in the preparation of organic solar cells [26].

In summary, the average device parameters ( $V_{oc}$ ,  $J_{sc}$ , FF, PCE) of the thin film organic solar cells based on P3HT:PCBM active layer with and without solvent additives are plotted in Fig. 4. Generally, the device whose active layer was mixed with DIO outperformed the rest of the active layers in most of the device parameters except open circuit voltages (Table 3). The mean power conversion efficiency was 2.74 % which is nearly 46 % higher than the reference cell and 19 % increase from CN additives. The enhancements in PCE after adding DIO and CN were mostly contributed by the improved photocurrent and FF.

However, the devices that were prepared using DMSO processing solvent additive exhibited poor  $J_{sc}$  and FF leading to a lowest recorded PCE in this experiment. These could be mainly due to the poor miscibility between P3HT and PCBM blend in the presence of DMSO which resulted in heterogeneous phase separation in the photoactive medium. The observed high open circuit voltages in

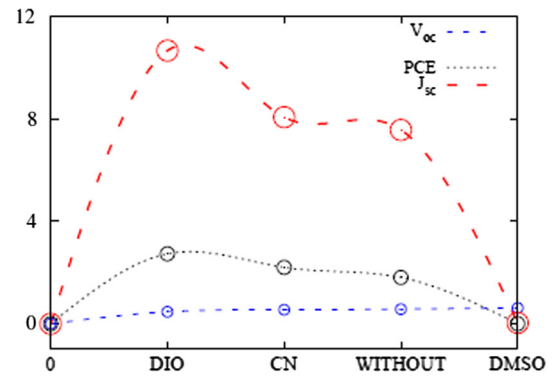


**Fig. 4** Average device parameters as a function of processing solvent additives

DMSO based thin film organic solar cell is an indication for high charge carrier recombination in the medium [25–28]. Improved device performance with additive is attributed to enhanced miscibility of the polymer molecules and increased degree of crystallization which has facilitated enhanced transport of charges in the medium.

## 4 Surface morphologies of the photoactive layers

The surface morphology of the photoactive films were studied using scanning electron microscope (SEM). The effect of solvent additives on the films morphologies of P3HT:PCBM are found to be directly correlated with device performance based on electrical measurements. Energy Dispersive X-ray Spectroscopy (EDX) was also conducted on the SEM images to identify the contents of the different features on the films surfaces. The SEM images as depicted in Fig. 5 evidently show the various patterns involving P3HT polymer chain and the distribution of PCBM in the medium. According to the EDX data from the islands of the surface morphology indicated that the lighter spots are rich in P3HT while the darker spots are rich in PCBM. The images taken from the surface of the film without solvent additive are appeared to have certain distribution spots in smooth background which are associated with the presence of P3HT clusters on the surface. However, in the case of the film produced with DIO (Fig. 5(2)), no sign of defect clusters have been recorded which suggests that the phase segregation between P3HT and PCBM domains in the film containing DIO processing solvent additive leads to much finer phase separation between the two molecules without large aggregates of PCBM or P3HT. This small-scale phase separation between the two molecules contributed to large value of  $J_{sc}$ .

**Table 3** Photovoltaic parameters of the four different organic thin film solar cell devices based on the blend of P3HT:PCBM active layer prepared with different organic solvent mixture

P3HT:PCBM	Voc (V)	Jsc (mA/cm <sup>2</sup> )	FF (%)	PCE (%)	Rs. (ohms)
CF with DIO (3%)	0.47	10.7	55	2.74	128
CF with CN (3%)	0.55	8.6	50	2.34	709
CF without additive	0.57	7.7	43	1.88	568
CF with DMSO (1%)	0.62	0.04	15	0.003	40,792

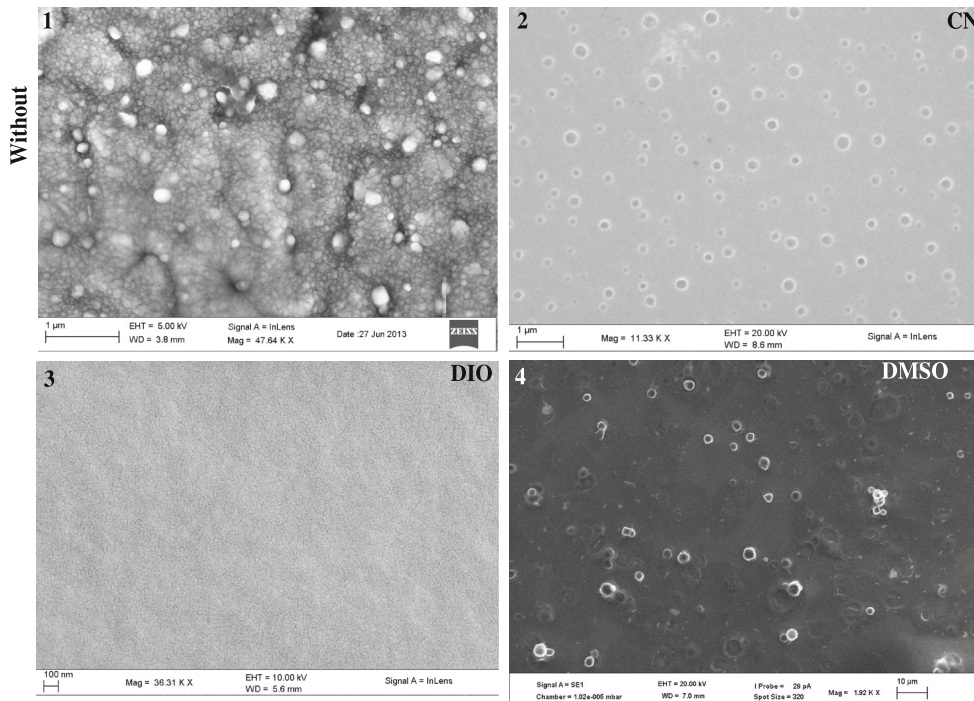


**Fig. 5** The SEM surface morphology of the films of P3HT:PCBM blend prepared with **1** without additive, **2** with DIO, **3** CN and **4** with DMSO

In contrast, the film surface containing CN (Fig. 5(1)) additive exhibited large concentration of PCBM or/and PCBM/P3HT clusters on the surface which creates undesirable traps for the free charge carriers that can hinder smooth charge transport across the medium. In spite of the presence of such large defect clusters, in the film with CN, the performance of the devices are found to be better than film (1) and (4). The SEM image of the P3HT:PCBM film prepared with DMSO (Fig. 5(4)), shows heterogeneous nanostructures with formation of large clusters on the surface of the film. The poor phase separation and formation of clusters as indicated (Fig. 5(4)) unfavorably reduces the formation of donor and acceptor interfaces in the medium which resulted in poor device performance. The surface morphology once again confirmed the existence of interpenetrating network of P3HT and PCBM in the photoactive layer which is responsible for efficient charge separation and transport. However, the photoactive medium with large clusters of the phase separated domains (e.g film with DMSO) the devices appeared to lose performance.

### 4.1 Charge transport properties

The charge transport properties of the photoactive layers composed of P3HT:PCBM with and without processing additives are discussed based on space charge limited current (SCLC) taken under dark condition. In a steady state condition, where the traps in the medium are filled, the space charge current obeys Mott–Gurney law which can be expressed as:

$$J_{SCL} = \frac{9}{8} \epsilon \epsilon_0 \mu_0 \exp(\gamma \sqrt{V/L}) \frac{V^2}{L^3} \tag{1}$$

Pole–Frenkel type field-dependent mobility (FDM) equation ( $\mu = \mu_0 \exp(\gamma \sqrt{E})$ ) is employed to describe the transport of charges in defect free medium. The relative permittivity was taken to be  $\epsilon = 3$  which is within the range of (3–5) for many polymers and the active layer thickness in this experiment was  $L = 120$  nm. The space charge limited currents data taken from the TFOSCs prepared under four types active layers were compared with the current density Eq. (1). According to the results

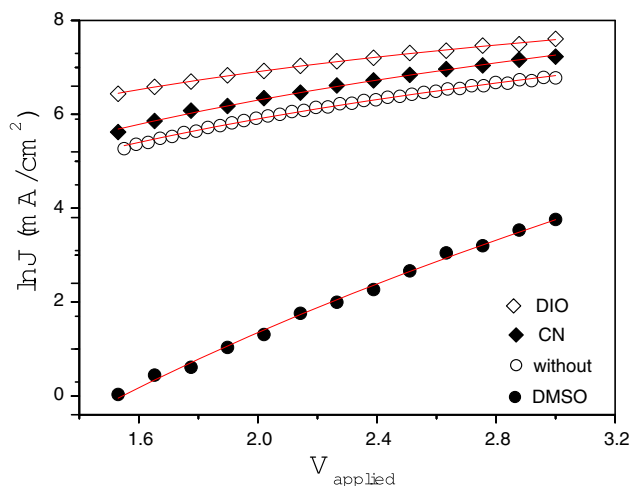


**Fig. 6** Space charge limited current of TFOSCs prepared with and without solvent additives. The *solid lines* are computer fits according to Eq. (1) to SCLC data taken from four different TFOSCs

displayed in Fig. 6 the trap free space charge limited equation agree very well with the data. There are clear evidences that the hole mobility obtained from DIO based devices is better than those with CN, DMSO or without additive. The highest mobilities recorded for best charge transport in organic medium are in the range of  $0.1 \text{ cm}^2 \text{ V}^{-1} \text{ s}^{-1}$  [29, 30]. The zero field mobilities and activation factor derived from fits to the data suggest that the film with DIO has the highest value followed by CN, without additive and DMSO, respectively. This improvement in hole mobility could be attributed to the fact that PCBM dissolves better in DIO solvent and increases the miscibility of the blend with P3HT, which makes P3HT to neatly arrange itself into ordered domains, avoiding excessive aggregation [2, 9, 10, 13, 29–31]. Meanwhile, we also noted that the mobility of the blend with CN based device is better than those without additive this is due to the high boiling point of CN which allows longer time for the distribution of PCBM into P3HT and delays P3HT molecules to self-assemble into highly ordered structure which enables high hole mobility and consequently a better fill factor (Table 4).

**Table 4** Summary of the transport parameters

P3HT:PCBM	$\mu_0$ ( $\text{cm}^2 \text{ V}^{-1} \text{ s}^{-1}$ )	$\gamma$ ( $\text{cm V}^{-1/2}$ )
CF without additive	$1.83 \times 10^{-5}$	$1.56 \times 10^{-2}$
CF with DIO (3 vol%)	$1.65 \times 10^{-4}$	$-1.35 \times 10^{-2}$
CF with CN (3 vol%)	$2.40 \times 10^{-5}$	$2.07 \times 10^{-2}$
CF with DMSO (1 vol%)	$3.14 \times 10^{-9}$	$1.88 \times 10^{-1}$

## 5 Conclusion

Organic thin film solar cells with and without processing solvent additives have been fabricated and characterized under ambient laboratory atmosphere. We have employed here three types of solvent additives DIO, CN and DMSO in chloroform based host solvent in order to be able to compare the miscibility of the P3HT:PCBM blend. According to the electrical measurements taken from the devices, the performance of the film mixed with DIO solvent outperforms all other variety of solvent additives used in this investigation. We have recorded device parameters as high as  $J_{sc} = 11 \text{ mA/cm}^2$ ,  $V_{oc} = 0.47 \text{ V}$ ,  $\text{FF} = 60 \%$  and  $\text{PCE} \approx 2.8 \%$  with DIO which are far better than those devices without solvent additive. These results show that the power conversion efficiency has grown by 46 % and the fill factor by 33 % by using 3 % DIO solvent additive in P3HT:PCBM blend. The second best performing thin film organic solar cell was those devices whose active layer was diluted with 1-chloronaphthalene (CN) solvent additive. In this case, the power conversion efficiency increased to 2.34 % which is nearly a 25 % growth from the reference cell. However, we found very low performance from those devices based on DMSO solvent additives. All the device parameters measured from DMSO based active layer were found to be well below the devices without solvent additive.

We found strong correlation between the uniformity of the film on one hand and device performance on the other according to the film morphologies investigated using SEM. The film surface with DIO appeared to be defect free and smooth compared to all other devices prepared in this investigation. This suggests that chloroform : DIO solvents mixture could have favored the formation of good interpenetrating network which positively impacted the charge transport process across the film. In fact, the space charge limited current investigated in this work compliment with the same conclusion which confirms that DIO based devices have the highest charge mobility than all the other devices. The relative higher boiling point of CN ( $250^\circ\text{C}$ ) than DIO ( $168^\circ\text{C}$ ) could have caused slow crystallization process of P3HT polymer which presumably influence the nanomorphology of the film.

**Acknowledgments** This work is partially supported by National Research Foundation (NRF) (Grant Numbers 92786, 93562 and 85589), South Africa. The authors are also thankful to members of staffs at Microscopy and Microanalysis Unit (MMU) in UKZN.

## References

1. R. Po, C. Carbonera, A. Bernardi, F. Tinti, N. Camaioni, *Solar Energy Mater. Solar Cells* **100**, 97 (2012)

2. J. Lee, W. Ma, C.J. Brabec, J. Yuen, J.S. Moon, J.Y. Kim, K. Lee, G. Bazan, A.J. Heeger, *J. Am. Chem. Soc.* **130**, 3619–3623 (2008)
3. L. Lu, T. Xu, I.H. Jung, L. Yu, *J. Phys. Chem. C* **118**, 22834–22839 (2014)
4. S.P. Cho, J.S. Yeo, D.Y. Kim, S. Na, S.S. Kim, *Solar Energy Mater. Solar Cells* **132**, 196–203 (2015)
5. X. Bao, Q. Zhu, T. Wang, J. Guo, C. Yang, D. Yu, N. Wang, W. Chen, R. Yang, *A.C.S. Appl. Mater. Interfaces* **7**, 7613–7618 (2015)
6. K. Zilberberg, J. Meyerb, T. Ried, *J. Mater. Chem. C* **1**, 4796–4815 (2013)
7. E.A.A. Arbab, B. Teleatu, G.T. Mola, *J. Mod. Opt.* **61**(21), 1749–1753 (2014)
8. C. Gong, H.B. Yang, Q.L. Song, C.M. Li, *Org. Electron.* **13**, 7–12 (2012)
9. I. Hancox, L.A. Rochford, D. Clare, M. Walker, J.J. Mudd, P. Sullivan, S. Schumann, C.F. McConville, T.S. Jones, *J. Phys. Chem. C* **117**, 49–57 (2013)
10. H.Q. Wang, N. Li, N.S. Guldal, C.J. Brabec, *Org. Electron.* **13**, 3014–3021 (2012)
11. T. Stubhan, T. Ameri, M. Salinas, J. Krantz, F. Machui et al., *Appl. Phys. Lett.* **98**, 253308 (2011)
12. J.M. Yun, J.S. Yeo, J. Kim, H.G. Jeong, D.Y. Kim, Y.J. Noh, S.S. Kim, B.C. Ku, S.I. Na, *Adv. Mater.* **23**, 4923–4928 (2011)
13. Y. Kwon, Y. Kim, H. Lee, C. Lee, J. Kwak, *Org. Electron.* **15**, 1083–1087 (2014)
14. M.C. Abramo, C. Caccamo, M. Calvo, V.C. Nibali, D. Costa, R. Giordano, G. Pellicane, R. Ruberto, U. Wanderlingh, *Philos. Mag.* **91**, 2066–2076 (2011)
15. G. Pellicane, O.D. Pandaram, *J. Chem. Phys.* **141**, 044508 (2014)
16. F. Zhang, K.G. Jespersen, C. Björström, M. Svensson, M.R. Andersson, K. Sundström, E. Moons, A. Yartsev, O. Inganäs, *Adv. Funct. Mater.* **16**, 667–674 (2006)
17. Y. Yao, J. Hou, Z. Xu, G. Li, Y. Yang, *Adv. Funct. Mater.* **18**, 1783–1789 (2008)
18. J. Peet, J.Y. Kim, N.E. Coates, W.L. Ma, D. Moses, A.J. Heeger, G.C. Bazan, *Nat. Mater.* **6**, 497–500 (2007)
19. J.S. Moon, C.J. Takacs, S. Cho, R.C. Coffin, H. Kim, G.C. Bazan, A.J. Heeger, *Nano Lett.* **10**, 4005–4008 (2010)
20. J.T. Rogers, K. Schmidt, M.F. Toney, E.J. Kramer, G.C. Bazan, *Adv. Mater.* **23**, 2284–2288 (2011)
21. Z. Ma, E. Wang, M.E. Jarvid, P. Henriksson, O. Inganäs, F. Zhang, M.R. Andersson, *J. Mater. Chem.* **22**, 2306–2314 (2012)
22. L. Li, H. Tang, H. Wu, G. Lu, X. Yang, *Org. Electron.* **10**, 1334–1344 (2009)
23. B. Nandan, L.D. Kandpal, G.N. Mathur, *Appl. Polym. Sci.* **90**, 2906–2918 (2003)
24. J. Peet, N.S. Cho, S.K. Lee, G.C. Bazan, *Macromolecules* **41**, 8655–8659 (2008)
25. G. Tessema, N. Abera, *Phys. B Condens. Matter* **445**, 56–59 (2014)
26. M. Vosgueritchian, D.J. Lipomi, Z. Bao, *Adv. Funct. Mater.* **22**, 421–428 (2012)
27. K. Vandewal, A. Gadisa, W.D. Oosterbaan, S. Bertho, F. Banishoeib, I.V. Severen, L. Lutsen, T.J. Cleij, D. Vanderzande, J.V. Manca, *Adv. Funct. Mater.* **18**, 2064–2070 (2008)
28. G. Tessema, *Appl. Phys. A Mater. Sci. Process.* **106**, 53 (2012)
29. H. Zhou, Y. Zhang, J. Seifert, S.D. Collins, C. Luo, G.C. Bazan et al., *Adv. Mater.* **25**, 4636–4643 (2013)
30. O. Ramirez, V. Cabrera, L.M. Resndiz, *Opt. Quant. Electron.* **46**, 1291–1296 (2014)
31. F.C. Chen, H.C. Tseng, C.J. Ko, *Appl. Phys. Lett.* **92**, 103316 (2008)